



This is a repository copy of *Direct yaw-moment control of an in-wheel-motored electric vehicle based on body slip angle fuzzy observer*.

White Rose Research Online URL for this paper:
<http://eprints.whiterose.ac.uk/8642/>

Article:

Geng, C., Mostefai, L., Denai, M. et al. (1 more author) (2009) Direct yaw-moment control of an in-wheel-motored electric vehicle based on body slip angle fuzzy observer. IEEE Transactions on Industrial Electronics, 56 (5). pp. 1411-1419. ISSN 0278-0046

<https://doi.org/10.1109/TIE.2009.2013737>

Reuse

Unless indicated otherwise, fulltext items are protected by copyright with all rights reserved. The copyright exception in section 29 of the Copyright, Designs and Patents Act 1988 allows the making of a single copy solely for the purpose of non-commercial research or private study within the limits of fair dealing. The publisher or other rights-holder may allow further reproduction and re-use of this version - refer to the White Rose Research Online record for this item. Where records identify the publisher as the copyright holder, users can verify any specific terms of use on the publisher's website.

Takedown

If you consider content in White Rose Research Online to be in breach of UK law, please notify us by emailing eprints@whiterose.ac.uk including the URL of the record and the reason for the withdrawal request.



eprints@whiterose.ac.uk
<https://eprints.whiterose.ac.uk/>

Direct Yaw-Moment Control of an In-Wheel-Motored Electric Vehicle Based on Body Slip Angle Fuzzy Observer

Cong Geng, Lotfi Mostefai, Mouloud Denai, and Yoichi Hori, *Fellow, IEEE*

Abstract—A stabilizing observer-based control algorithm for an in-wheel-motored vehicle is proposed, which generates direct yaw moment to compensate for the state deviations. The control scheme is based on a fuzzy rule-based body slip angle (β) observer. In the design strategy of the fuzzy observer, the vehicle dynamics is represented by Takagi–Sugeno-like fuzzy models. Initially, local equivalent vehicle models are built using the linear approximations of vehicle dynamics for low and high lateral acceleration operating regimes, respectively. The optimal β observer is then designed for each local model using Kalman filter theory. Finally, local observers are combined to form the overall control system by using fuzzy rules. These fuzzy rules represent the qualitative relationships among the variables associated with the nonlinear and uncertain nature of vehicle dynamics, such as tire force saturation and the influence of road adherence. An adaptation mechanism for the fuzzy membership functions has been incorporated to improve the accuracy and performance of the system. The effectiveness of this design approach has been demonstrated in simulations and in a real-time experimental setting.

Index Terms—Fuzzy observer, local modeling, state feedback, vehicle lateral dynamics.

I. INTRODUCTION

THIS PAPER focuses on the design of control strategies to enhance the performance and safety of electric vehicles (EVs) in critical driving situations. It has been commonly recognized that EVs are inherently more suitable to realize active safety stability control over conventional internal combustion engine vehicles. In EVs, the motor torque can be measured and controlled accurately, and in-wheel motors can be installed in each EV's rear and front tires. Based on these structural merits, vehicle motion can be stabilized by additional yaw moment generated as a result of the difference in tire driving or braking forces between the right and left sides of the

Manuscript received June 15, 2008; revised January 6, 2009. First published February 6, 2009; current version published April 29, 2009.

C. Geng is with the University of Tokyo, Tokyo 113-8656, Japan (e-mail: geng@horilab.iis.u-tokyo.ac.jp).

L. Mostefai is with the University Moulay Tahar in Saida, Saida 20000, Algeria.

M. Denai is with Mohamed Boudiaf University of Science and Technology of Oran, Oran 31000, Algeria, and also with the Department of Automatic Control and Systems Engineering, The University of Sheffield, Sheffield, S1 3JD, U.K.

Y. Hori is with the Department of Informatics and Electronics, Institute of Industrial Science, University of Tokyo, Tokyo 153-8505, Japan.

Color versions of one or more of the figures in this paper are available online at <http://ieeexplore.ieee.org>.

Digital Object Identifier 10.1109/TIE.2009.2013737

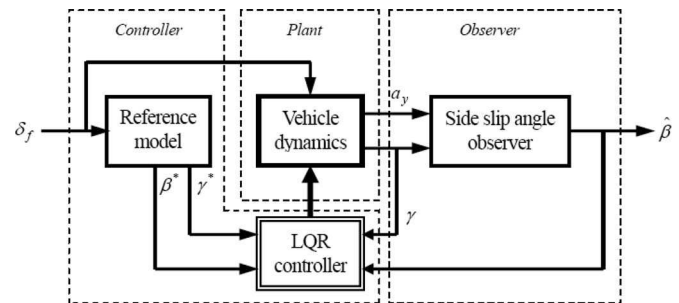


Fig. 1. Vehicle lateral stability control structure.

vehicle, which is the so-called “Direct Yaw-moment Control” (DYC) [1]–[5].

Fig. 1 shows the main concept of the chassis control system utilizing DYC based on the model matching control method and optimal control method [3], [4], [6].

This system is aimed to maintain the driver's handling ability at the physical limit of adhesion between the tires and the road by making the vehicle easily controllable even well below that limit. The dynamics of the 2-DOF vehicle model can describe the driver's familiar characteristics under normal driving conditions. The body slip angle (β) and yaw rate (γ) calculated from the model are taken as the desired behavior of the vehicle. By applying the model matching control, the yaw-moment optimal decision can be derived from the deviations of the state feedback compensator of β and γ from their desired values. Since sensors for the direct measurement of β are very expensive, the construction of an observer for its estimation is desirable.

Generally, such state feedback control method is based on the state equations derived from the vehicle dynamics. However, the implementation of these techniques is still difficult since the vehicle dynamics is highly nonlinear, particularly for β . Previous authors' approaches regarding β estimation issue used model-based observers with either linear or nonlinear equivalent vehicle dynamic models [6]–[10]. With regard to linear observer design, the linear 2-DOF vehicle model with fixed parameters is adopted. However, this approach cannot always achieve accurate results in different running situations. In the design of nonlinear observers, tire characteristics are described by nonlinear functions and with more parameters, which can produce relatively more accurate results in different running situations compared with linear observers. However, nonlinear observers have the disadvantages of not having a

strong theoretical maturity and still face difficulties regarding their real-time implementation.

The main nonlinearity of vehicle dynamics comes from the tire force saturation imposed by the limits of tire adherence, which makes β response change considerably if the vehicle is cornering much more than usual. In other words, the model structure or parameters should vary according to the different operating regimes for a more practical controller design. In addition, the nonlinear nature of vehicle dynamics is further complicated by the influence of the characteristics of whole chassis elements (tires, suspensions, and steering system). It is hard to determine the physical model parameters theoretically. Therefore, an effective modeling methodology is the key for the system design.

To deal with the difficulties associated with nonlinearity modeling, as well as to make use of the linear observer advantages such as simplicity in the design and implementation, the nonlinear vehicle dynamics is represented by Takagi–Sugeno (T–S) fuzzy models [11], [12]. The local approximation of the nonlinear vehicle model and a dynamical interpolation method are introduced in this paper to construct a fuzzy-model-based control system for β estimation and control. Optimal β observer is designed for each local model using Kalman filter theory. The proposed system is a combination of local linear observers and controllers with varying switching partition.

The first step in the design is concerned with the derivation of the system state equations from the vehicle dynamics and local approximation of nonlinear tire model. These modeling techniques are considered appropriate for online control system design (linear 2-DOF vehicle model as in [13]). In the next step, a fuzzy-based modeling approach is used to get a hybridlike vehicle model, which is calculated as a weighted sum of the outputs of two local linear models. For practical applications, parameter identification is conducted experimentally. An adaptation mechanism of the fuzzy membership functions has been included to make the model fit different running conditions and road friction changes. The membership functions of the weighting factors are chosen to be dependent on lateral acceleration and road friction coefficient. The two local observers are based on local linear tire models, which inherently leads to a relatively simple design, and have been combined into a single overall observer by means of fuzzy rules. Furthermore, the nonlinear global system results show high β estimation capabilities and good adaptation to changing road friction. A series of simulations are performed to evaluate the effectiveness of the proposed β observer when incorporated into a DYC-based control scheme.

II. VEHICLE DYNAMICS AND FUZZY MODELING

A. Local Approximation and Linearization of Vehicle Dynamics

The system is based on an in-wheel-motored EV dynamic model (Fig. 2). The main difference with common vehicle dynamics is that the direct yaw moment is an additional input variable, which is caused by individual motor torque between each wheel.

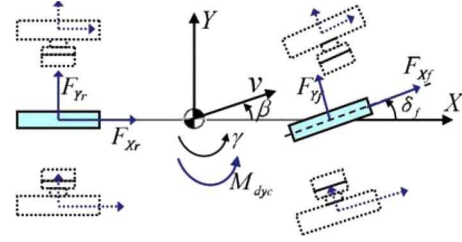


Fig. 2. Two-DOF vehicle model.

The vehicle dynamics is approximately described by the following 2-DOF vehicle model equations:

$$\begin{cases} ma_y = F_{xf} \sin \delta_f + F_{yf} \cos \delta_f + F_{yr} \\ I_z \dot{\gamma} = l_f F_{xf} \sin \delta_f + l_f F_{yf} \cos \delta_f - l_r F_{yr} + N \end{cases} \quad (1)$$

where a_y denotes the vehicle lateral acceleration, γ is the yaw rate, δ_f is the steering angle of the front wheel, N is the direct yaw moment, m represents the mass of the vehicle, I_z is the yaw inertia moment, l_f denotes the distance between the center of the mass and the front axle, l_r is the distance between the center of mass and the rear axle, F_{xf} is the longitudinal force of the front tires, and F_{yf} and F_{yr} are the lateral forces of the front and rear tires, respectively.

Let the body slip angle β and yaw rate γ represent the system state variables. By defining the kinematics relationship as $a_y = v(\dot{\beta} + \gamma)$ and assuming that δ_f is relatively small for high speeds, the vehicle's state equations are obtained as follows:

$$\begin{cases} \dot{\beta} = \frac{1}{mV} (F_{yf} + F_{yr}) - \dot{\gamma} \\ \dot{\gamma} = \frac{1}{I_z} (l_f F_{yf} - l_r F_{yr} + N). \end{cases} \quad (2)$$

The model of (2) is nonlinear due to the tire lateral force dynamics. By using local operating regime approximations, the model can be simplified into an equivalent linear 2-DOF model by adopting the equivalent tire cornering stiffness C , which is defined by

$$C = \frac{F_y}{\alpha} \quad (3)$$

where F_y is the tire lateral force, and α is the tire slip angle at its operating point.

By adopting the value of C given by (3), the nonlinear vehicle dynamic state equation (2) can be transformed into the following equivalent linear state equation at the local operating point:

$$\dot{x} = Ax + Bu \quad (4)$$

in which

$$\mathbf{A} = \begin{bmatrix} a_{11} & a_{12} \\ a_{21} & a_{22} \end{bmatrix} = \begin{bmatrix} \frac{-(2C_f + 2C_r)}{mV} & \frac{-2l_f C_f + 2l_r C_r}{mV^2} - 1 \\ \frac{-2l_f C_f + 2l_r C_r}{I_z} & \frac{-2l_f^2 C_f - 2l_r^2 C_r}{I_z V} \end{bmatrix}$$

$$\mathbf{B} = \begin{bmatrix} b_{11} & b_{12} \\ b_{21} & b_{22} \end{bmatrix} = \begin{bmatrix} \frac{2C_f}{mV} & 0 \\ \frac{2l_f C_f}{I_z} & \frac{1}{I_z} \end{bmatrix}$$

$$x = \begin{bmatrix} \beta \\ \gamma \end{bmatrix} \quad u = \begin{bmatrix} \delta_f \\ N \end{bmatrix}$$

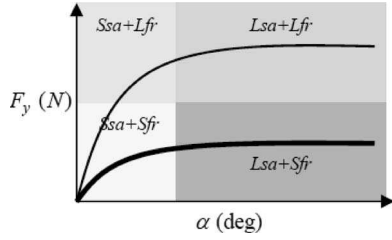


Fig. 3. Tire lateral force characteristics partitioned roughly into four different local dynamics (Lsa is the large tire slip angle, Ssa is the small tire slip angle, Lfr is the large friction, and Sfr is the small friction).

where C_f and C_r are the cornering stiffness values of the front and rear tires, respectively, and V is the longitudinal velocity.

Since the main nonlinearity in the model comes from the tires, the cornering stiffness of the tires will play an important role in the formulation of the model used in the estimator. According to Fig. 3, these coefficients are large when the tire slip angle assumes small values, which are equivalent to the low lateral acceleration regimes. On the other hand, the stiffness coefficients become small when the tire slip angle increases, which means that the vehicle is running at high lateral accelerations. Hence, to describe the vehicle dynamics by an equivalent linear 2-DOF model, local models with different C values should be considered, for both low and high lateral accelerations.

B. Model Parameter Identification

For the local dynamic models, the equivalent tire cornering stiffness values C_f and C_r are difficult to determine theoretically because they are influenced by the suspension dynamics, tire characteristics, and steering system. In this paper, an identification method of tire cornering stiffness based on experimental tests performed on the EV is proposed.

According to (2), the steady state cornering relationship with steering angle input can be expressed as follows:

$$\begin{cases} ma_y = F_{yf} + F_{yr} \\ 0 = l_f F_{yf} - l_r F_{yr}. \end{cases} \quad (5)$$

From (5), the expression of the side force applied to the front and rear tires can be deduced as

$$\begin{cases} \hat{F}_{yf} = \frac{l_r}{l} ma_y \\ \hat{F}_{yr} = \frac{l_f}{l} ma_y. \end{cases} \quad (6)$$

Moreover, the body slip angle of front and rear tires can be obtained as

$$\begin{cases} \hat{\alpha}_f = \beta + \frac{\gamma l_f}{V} - \delta_f \\ \hat{\alpha}_r = \beta - \frac{\gamma l_r}{V}. \end{cases} \quad (7)$$

If a_y , β , and γ are measured from steady state cornering experiments, it follows from the aforementioned equations that the tire cornering stiffness can be obtained as

$$\begin{cases} \hat{C}_f = \frac{F_{yf}}{-2\alpha_f} \\ \hat{C}_r = \frac{F_{yr}}{-2\alpha_r}. \end{cases} \quad (8)$$

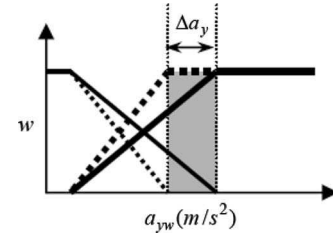


Fig. 4. Membership function adaptation to the lateral acceleration.

For the nonlinearity of vehicle dynamics, cornering experiments with low and high a_y 's should be conducted, respectively, to identify the different cornering stiffness values in different operating regimes.

C. Fuzzy Modeling and Local Dynamics

To simplify the fuzzy modeling procedure, the lateral acceleration a_y will be assigned two fuzzy sets (large and small), as shown in Fig. 4.

Then, using these fuzzy sets, the fuzzy IF-THEN rules for the vehicle dynamic model can be defined as follows.

Rule i : (local model i) IF $|a_y|$ is F_i , THEN $\dot{x} = A_i x + B_i u$.

The overall vehicle dynamics is described by two models that take the form of (4). The model parameters, namely, the equivalent tire cornering stiffness, are identified according to the steady state regime given by (8).

For the local model 1, the tire works at its small slip region, and A_1 and B_1 are calculated based on the largest value of the cornering stiffness C . For the local model 2, the tire works at its large slip region, and A_2 and B_2 are calculated for a relatively small value of the cornering stiffness C .

Finally, the whole nonlinear dynamics of the vehicle are described with the proposed dynamic switching partition by interpolating the two models with fuzzy logic. By a proper choice of the membership function, the vehicle dynamics can be calculated for different operating regimes (from low to high a_y value).

Therefore, the following is used to represent the fuzzy models covering the vehicle dynamics:

$$\dot{x} = \sum_{i=1}^2 w_i (A_i x + B_i u) \quad (9)$$

where w_1 and w_2 are the membership functions for local models 1 and 2. For design simplicity, trapezoidal membership functions have been used. The formulations of $w_1(a_y)$ and $w_2(a_y)$ are as follows:

$$w_1(a_y) = \begin{cases} 1 - \frac{1}{a_{yw}} a_y, & |a_y| \leq a_{yw} \\ 0, & |a_y| > a_{yw} \end{cases} \quad (10)$$

$$w_2(a_y) = \begin{cases} \frac{1}{a_{yw}} a_y, & |a_y| \leq a_{yw} \\ 1, & |a_y| > a_{yw} \end{cases} \quad (11)$$

where the coefficient a_{yw} describes the value of a_y at the tire/road adherence limit (road friction coefficient μ) when the tire force is saturated, which is equivalent to severe steering dynamics.

Road condition is one of the most important factors that must be considered in vehicle dynamic stability control, since the road friction coefficient μ is uncertain and may change according to the road condition; the fuzzy partition describing the vehicle model must be adaptive to such variations (Fig. 4).

The value of μ can be identified with different methods. In EV stability control, one method that the authors adopted previously is to identify the μ value by analyzing wheel rotation dynamics, which takes advantage of the accurate knowledge of the EV motor torque values [14], [15]. With the identified μ value, a_{yw} is used as a tuning parameter of the weighting function partition to form an adaptation mechanism to cope with the variation of tire/road adherence conditions. In this paper, a_{yw} is set to be a linear function of μ with the following low-pass filter to remove the noise:

$$a_{yw} = k_{\mu} \frac{1}{1 + T_f s} \mu \quad (12)$$

where k_{μ} is the adaptation gain, and T_f is the constant of first order low-pass filter.

III. β OBSERVER DESIGN BASED ON FUZZY MODELS

A. Kalman Filter for Local β Observer Design

Based on the local linear models, the β observer is designed with Kalman filter theory [16]–[18]. For the real-time implementation of the design strategy, the continuous-time model of (4) is converted into discrete time model by taking into account process and measurement noises as follows:

$$\begin{aligned} x[n+1] &= G_i x[n] + H_i u[n] + \omega[n] \\ y[n] &= C_i x[n] + D_i u[n] + v[n] \end{aligned} \quad (13)$$

where the covariance vectors of process and measurement noises are assumed to be the same for all dynamics

$$E(\omega[n]\omega[n]^T) = Q \quad E(v[n]v[n]^T) = R. \quad (14)$$

The sampled equations with a zeroth-order hold are obtained as

$$\begin{aligned} G_i &= \begin{bmatrix} 1 + T_s a_{11} & T_s a_{12} \\ T_s a_{21} & 1 + T_s a_{21} \end{bmatrix} \\ H_i &= \begin{bmatrix} T_s b_{11} & T_s b_{12} \\ T_s b_{21} & T_s b_{21} \end{bmatrix} \end{aligned} \quad (15)$$

where T_s is the sampling time.

Using the discrete state space equation (13), a discrete form of Kalman estimator can be applied for each linear observer. The vehicle lateral acceleration a_y and yaw rate γ are two measurable variables and are chosen as output variables of the observer

$$\begin{aligned} y &= \begin{bmatrix} \gamma \\ a_y \end{bmatrix} \\ C &= \begin{bmatrix} 0 & 1 \\ \nu a_{11} & \nu(a_{12} + 1) \end{bmatrix} \\ D &= \begin{bmatrix} 0 & 0 \\ \nu b_{11} & 0 \end{bmatrix}. \end{aligned} \quad (16)$$

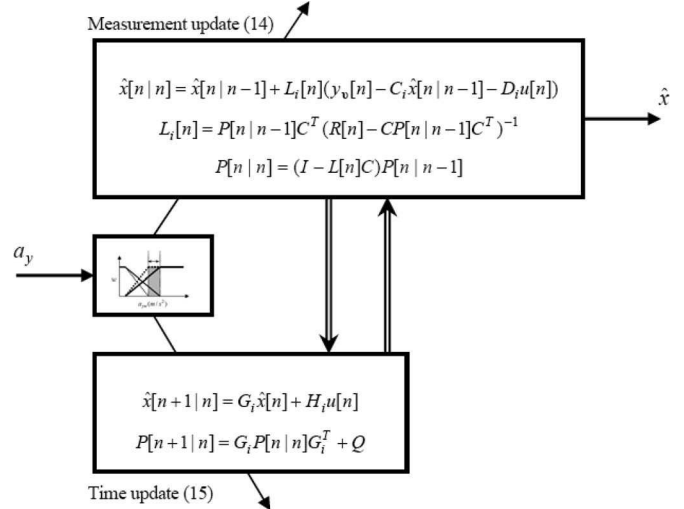


Fig. 5. Implementation of the estimation algorithm based on Kalman filter theory.

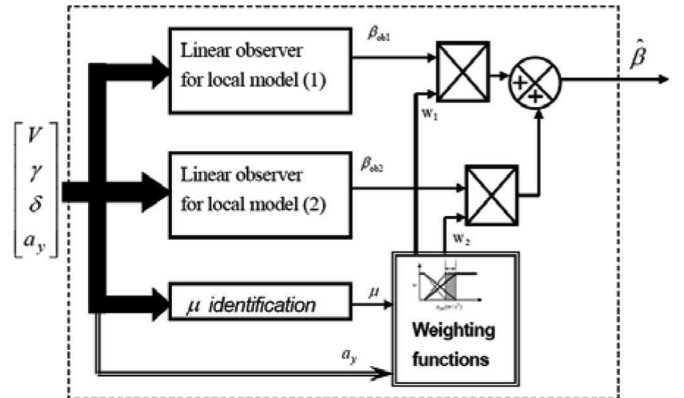


Fig. 6. Structure of hybrid adaptive observer.

The recursive discrete Kalman filter algorithm is then applied separately to estimate local dynamics, as shown in Fig. 5. Where \hat{x} and \hat{y} are the estimates of x and y , respectively, L_i is the feedback gain of local observer, which is derived using the Kalman filter theory.

B. Hybridlike Observer Design Based on Fuzzy Models

A hybridlike observer is designed based on the fuzzy discrete time vehicle models by applying the Kalman filter theory [9]. The proposed observer structure is as shown in Fig. 6.

The observer consists of two Kalman-filter-based local observers related to the aforementioned local models 1 and 2, respectively. The observer outputs are the estimates of β_{ob1} and β_{ob2} , respectively.

The fuzzy rules for β observer are defined by the following IF–THEN rule structure.

Rule i : (local observer i) IF $|a_y|$ is F_i , THEN $\hat{\beta}_{ob} = \hat{\beta}_{obi}$.

By introducing this fuzzy logic concept, two local linear models were sufficient to cover the main nonlinear features of the dynamics and give the proposed observer the ability to overcome the limitations associated with the linear observer

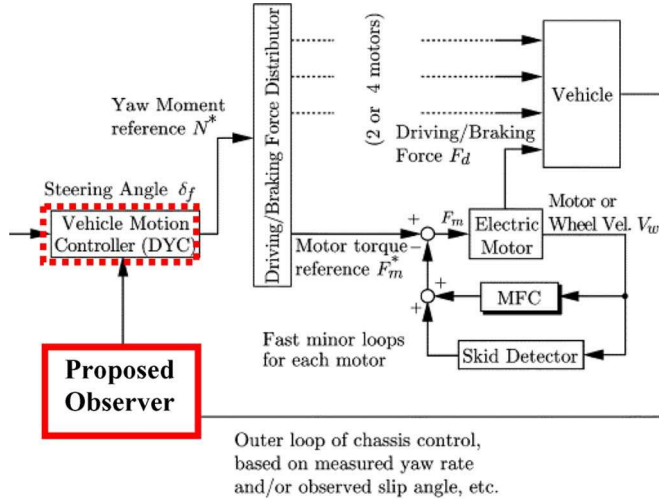


Fig. 7. Vehicle stability control applied to UOT MARCH II.

in terms of performances. The overall fuzzy observer is given by

$$\hat{\beta}_{ob} = \sum_{i=1}^2 w_i \hat{\beta}_{obi}. \quad (17)$$

The advantages of a linear observer such as simple design and noncomputationally intensive are conserved while addressing the nonlinear problem at the same time.

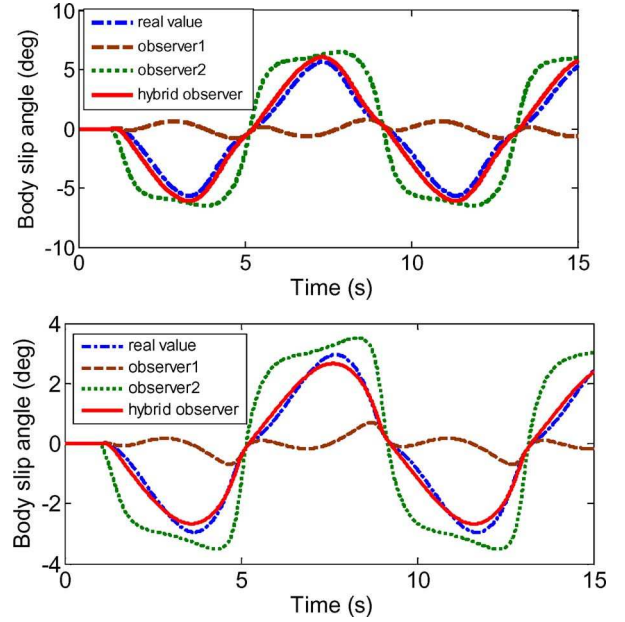
IV. SIMULATION AND EXPERIMENTAL RESULT ANALYSIS

A. Description of the Experimental Vehicle and Control Architecture

A full description of the EV University of Tokyo (UOT) MARCH II is presented in the Appendix. The parameters used in the following simulations and observer/controller design have been obtained in a previous study [19]. Fig. 7 shows the overall dynamical control scheme applied to UOT MARCH II. With reference to Fig. 1, we can clearly distinguish the parts which we have developed in this paper, namely, 1) the (red thick line) β observer already implemented and tested and 2) the (red dotted line) control to be tested in the near future for safety reasons. According to the configuration of the vehicle using four in-wheel motors, an optimal driving/braking force distribution system has been developed in former research to be applied with the DYC control unit [20].

B. Simulation and Experimental Studies of the Observer

The effectiveness of the proposed observer structure is tested via simulations. A sinusoidal steering angle input is chosen to simulate consecutive lane change maneuvers of the vehicle body. The amplitude of input steering angle is large enough to make the tire span both the linear and nonlinear working regions. Simulation results related to different road friction conditions are shown in Fig. 8. It is clear that both of the subobservers used to generate the proposed structure cannot fit well the real value for the whole operating conditions. This can


 Fig. 8. Simulation results of the hybrid observer under (top panel) large road friction situation ($\mu = 0.85$) and (bottom panel) small road friction situation ($\mu = 0.4$).

be explained by the fact that they are based on a local model with fixed parameters describing a limited segment of vehicle operating regime. Comparatively, the hybrid observer gives a better estimation, follows closely the real values, and has even the ability to adapt to different road friction conditions.

To evaluate the proposed control scheme under more realistic conditions, field tests are conducted on our experimental EV ‘‘UOT March II.’’ UOT March II is equipped with an acceleration sensor, a gyro sensor, and a noncontact speed meter, which provide measurements of the vehicle state variables.

Figs. 9 and 10 show the results of field tests of the observer in moderate and severe cornering situations. The experiments demonstrate that the observer is very effective and suitable for real-time applications due to its high onboard computational speed.

V. SIMULATION OF OPTIMAL YAW-MOMENT CONTROL BASED ON THE PROPOSED β OBSERVER

A. Desired Model and State Deviation Equation

As shown in Fig. 1, the control scheme is applied for DYC system design by using the model matching control method.

The desired state variables of β and γ are determined by a 2-DOF linear model with front wheel steering angle as input according to (4) and are expressed as follows:

$$\begin{bmatrix} \dot{\beta}_d \\ \dot{\gamma}_d \end{bmatrix} = A \begin{bmatrix} \beta_d \\ \gamma_d \end{bmatrix} + \begin{bmatrix} b_{11} \\ b_{21} \end{bmatrix} \delta_f. \quad (18)$$

In addition, γ should be constrained by its adhesion saturation value as follows:

$$\gamma_d \leq \frac{\mu g}{V}. \quad (19)$$

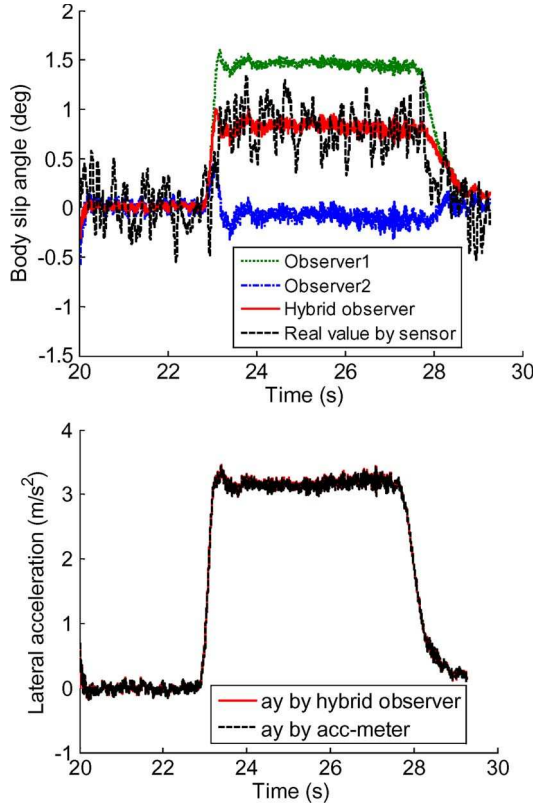


Fig. 9. Experimental field test results of β observer (steering angle = 90° ; $v = 40$ km/h).

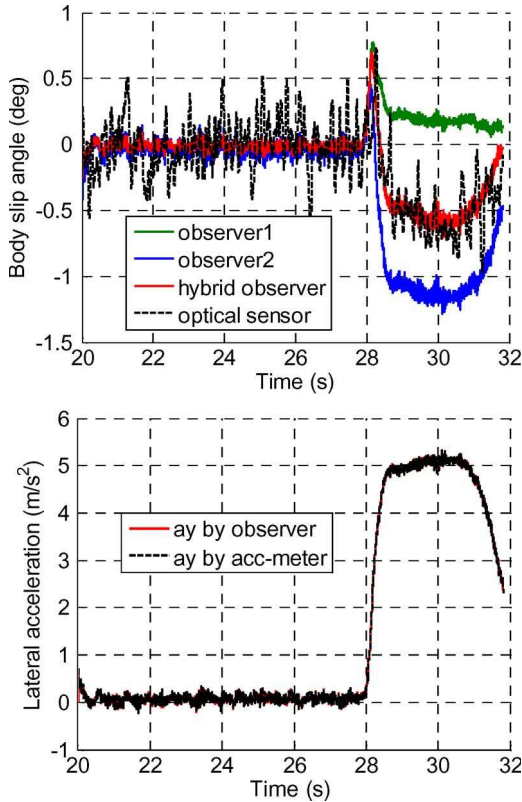


Fig. 10. Experimental field test results of β observer (steering angle = 90° ; $v = 60$ km/h).

The state deviation variable between the desired value X_d and actual value X is assumed to be as follows:

$$E = X - X_d = \begin{bmatrix} \Delta\beta \\ \Delta\gamma \end{bmatrix} = \begin{bmatrix} \beta - \beta_d \\ \gamma - \gamma_d \end{bmatrix}. \quad (20)$$

According to (4) and (18), the differentiation of (20) leads to the error dynamics

$$\dot{E} = \dot{X} - \dot{X}_d = A.E + \begin{bmatrix} b_{12} \\ b_{22} \end{bmatrix} N. \quad (21)$$

Equation (21) describes the dynamic relationship between the direct yaw moment and vehicle motion state deviations. It shows that, when a vehicle motion deviation appears, exerting a direct yaw moment can reduce them to make the vehicle regain stability.

B. Optimal Yaw-Moment Decision Algorithm

Based on the linear quadratic regulator method, the optimal control input can be calculated by state feedback deviations as follows:

$$N^* = -k_1(\beta - \beta_d) - k_2(\gamma - \gamma_d) \quad (22)$$

where the feedback gains k_1 and k_2 related to the local model are determined so that the following performance index is minimized:

$$J = \frac{1}{2} \int_0^\infty [q_1 \Delta\beta^2(t) + q_2 \Delta\gamma^2(t) + N^2(t)] dt \quad (23)$$

where q_1 and q_2 are the weighting coefficients of the state deviations, which can be chosen to modulate the controller sensitivity with respect to β and γ deviations. For this purpose, the coefficient ω_β ($0 \leq \omega_\beta \leq 1$) is introduced in the performance index as a weighting factor on β deviation. We define $q_1 = q^2 \omega_\beta$ and $q_2 = q^2 (1 - \omega_\beta)$, and (23) can be rewritten as

$$J = \frac{q}{2} \int_0^\infty [\omega_\beta \Delta\beta^2(t) + (1 - \omega_\beta) \Delta\gamma^2(t) + N^2(t)] dt. \quad (24)$$

Small values of β produce a more important γ matching control, whereas larger values lead to a more important β control. In addition, the vehicle stability is more sensitive to β deviation under low adhesion road conditions than it is under high adhesion road conditions. Therefore, ω_β is dependent on β and the road friction coefficient μ and is chosen as follows:

$$\omega_\beta = \begin{cases} \frac{|\beta|}{\mu \cdot \beta_0}, & \text{if } |\beta| < \mu \cdot \beta_0 \\ 1, & \text{else} \end{cases} \quad (25)$$

where β_0 is a threshold value which has been set to 10° based on the authors' experience.

The graph of ω_β as a function of β is shown in Fig. 11.

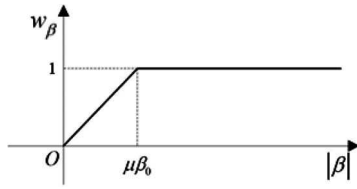


Fig. 11. Weight of body slip angle deviation for optimal yaw-moment decision.

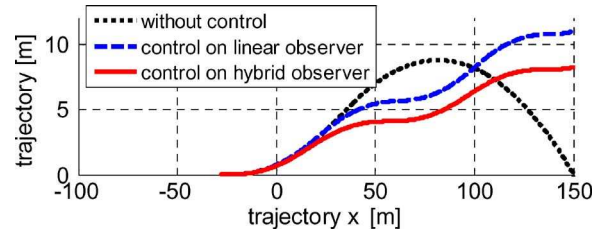


Fig. 13. Vehicle trajectory with and without β control.

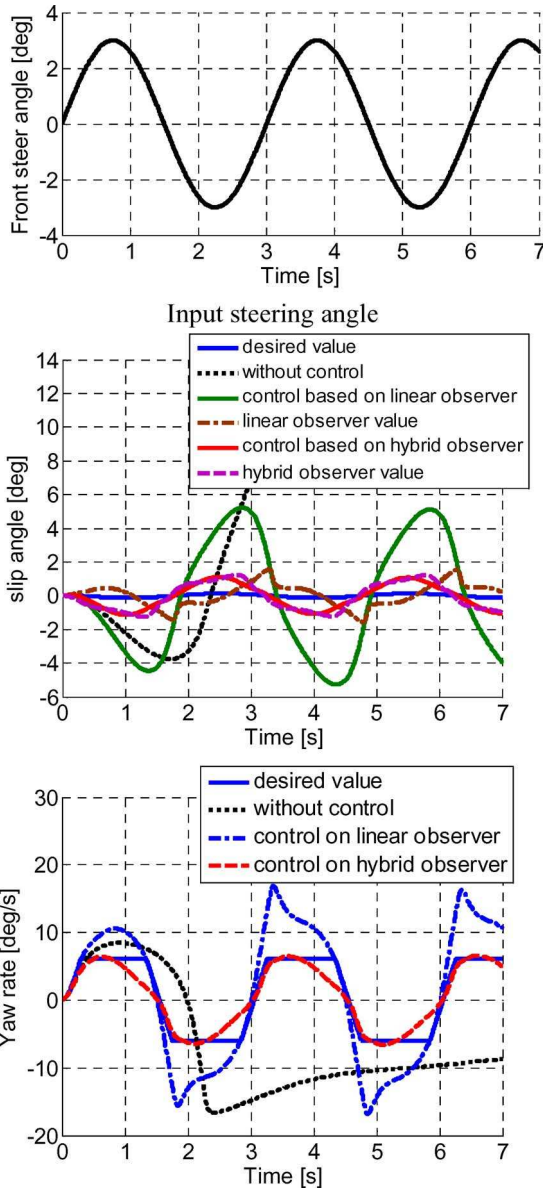


Fig. 12. (Top panel) Slip angle and (bottom panel) yaw rate under β control.

C. Simulation Results of Body Slip Angle Control

In the following simulations, full four-wheel vehicle dynamics with nonlinear tire model is used as a mathematical model.

In the simulation study and experimental validation, the actuation dynamics will not be considered. They rely essentially on the current control of electric motors. So far, it is well known that the use of electric motors as actuators is one of the advantages of EVs and, at the same time, presents a negligible

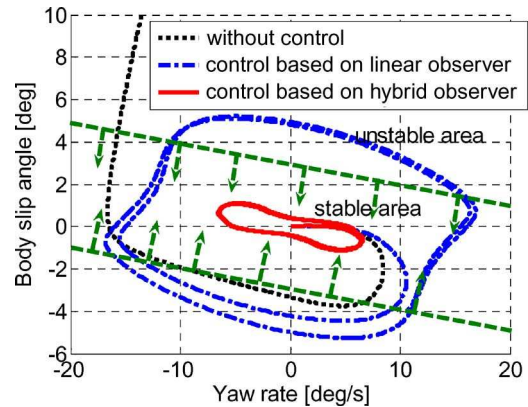


Fig. 14. Control trajectories in β - γ phase plane.

short delay (i.e., a few milliseconds) in the overall controlled system compared to the vehicle dynamics.

Fig. 12 shows the simulation results with sinusoidal front steering angle input when the road friction coefficient is 0.3 and the vehicle is running at a speed of 100 km/h. This can represent a critical driving situation of continuous lane change maneuver on slippery road. If the control is set off, β can assume larger values, causing the vehicle to lose its stability and unable to accomplish the lane change as in normal situations (Fig. 13). With the proposed hybrid observer, an accurate estimation of body slip angle is obtained. By applying DYC based on the hybrid observer, the yaw rate γ is successfully controlled to the desired value, and the body slip angle β is guaranteed to be limited. However, if DYC was based on the linear observer, the incorrect estimation of body slip angle will lead to control deterioration.

Fig. 14 shows the β - γ phase plane trajectory related to the simulation results. Under DYC control, a limited trajectory loop is drawn by the vehicle within the stable area defined for our vehicle. Without β control, this trajectory of β - γ phase plane cannot be satisfied and becomes much larger until the vehicle leaves the stable area, putting the passengers in danger.

VI. CONCLUSION

This paper has presented an algorithmic solution of the nonlinear vehicle dynamic control problem, which has been validated both in a simulation environment and in real time. A state observer has been designed for an in-wheel-motored EV with DYC using fuzzy modeling techniques. T-S fuzzy models were employed for approximating the nonlinear vehicle dynamics with linear local models. An adaptation mechanism was introduced to adjust the fuzzy membership functions in

TABLE I
SPECIFICATIONS OF UOT ELECTRIC MARCH II

Drivetrain	4 PM Motors / Meidensya Co.
Max. Power (20 sec.)	36 [kW] (48.3 [HP])*
Max. Torque	77* [Nm]
Gear Ratio	5.0
Battery	Lead Acid
Weight	14.0 [kg] (for 1 unit)
Total Voltage	228 [V] (with 19 units)
Base Chassis	Nissan March K11
Wheel Base	2360 [m]
Wheel Tread F/R	1365/1325 [m]
Total Weight	1400 [kg]
Wheel Inertia**	8.2 [kg]***
Wheel Radius	0.28 [m]
Controller	
CPU	MMX Pentium 233 [MHz]
Rotary Encoder	3600 [ppr]***
Gyro Sensor	Fiber Optical Type

* ... for only one motor. ** ... mass equivalent.
*** ... affected by gear ratio.

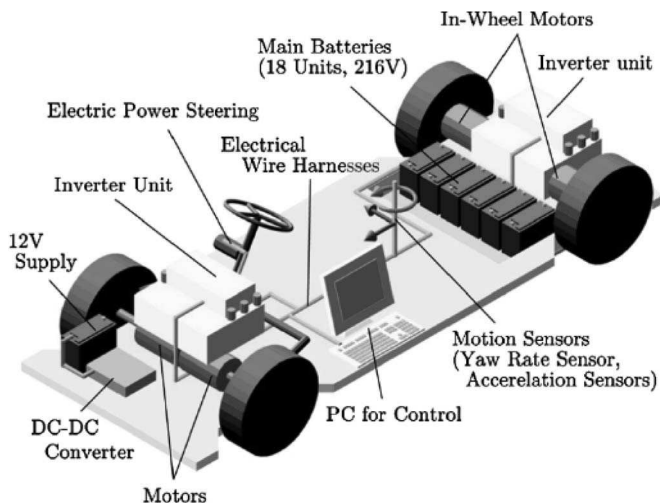


Fig. 15. Sketch of the "UOT MARCH II."

response to changes in road friction conditions. The local observer design was based on the Kalman filter theory and was combined with an interpolating mechanism which provided the link between the underlying local dynamics. The quantitative accuracy and the adaptation performance of the proposed observer have been verified in simulations and experimentally. We have shown that the designed controller relies critically on the estimated value of β , and further research and effort will be devoted into the implementation of a full dynamic stability control of the UOT MARCH II.

APPENDIX DESCRIPTION OF "UOT MARCH II"

The EV named "UOT Electric March II" was constructed in 2001 (Table I). The most special feature of this EV is the in-wheel motor mounted in each wheel. We can control each wheel torque completely and independently. Regenerative braking is also available. Former researchers from Hori Laboratory at the UOT contributed to build this EV by remodeling a Nissan March. Fig. 15 shows a sketch of the "UOT MARCH II."

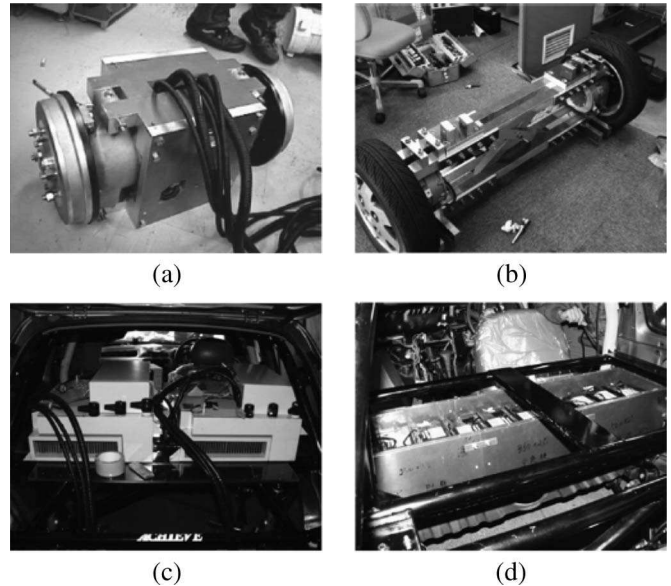


Fig. 16. Photographs of the vehicle. (a) Front motors. (b) Rear motors. (c) Inverters. (d) Batteries.

Fig. 16 shows the photographs of the main parts of the vehicle developed in our laboratory.

REFERENCES

- [1] Y. Hori, "Future vehicle driven by electricity and control research on 4 wheel motored 'UOT March II,'" in *Proc. 7th AMC*, 2002, pp. 1–14.
- [2] D. Kim, S. Hwang, and H. Kim, "Vehicle stability enhancement of four-wheel-drive hybrid electric vehicle using rear motor control," *IEEE Trans. Veh. Technol.*, vol. 57, no. 2, pp. 727–735, Mar. 2008.
- [3] K. Kin, O. Yano, and H. Urabe, "Enhancements in vehicle stability and steerability with slip control," *JSAE Rev.*, vol. 24, no. 1, pp. 71–79, Jan. 2003.
- [4] M. Canale, L. Fagiano, A. Ferrara, and C. Vecchio, "Vehicle yaw control via second-order sliding-mode technique," *IEEE Trans. Ind. Electron.*, vol. 55, no. 11, pp. 3908–3916, Nov. 2008.
- [5] N. Mutoh, Y. Hayano, H. Yahagi, and K. Takita, "Electric braking control methods for electric vehicles with independently driven front and rear wheels," *IEEE Trans. Ind. Electron.*, vol. 54, no. 2, pp. 1168–1176, Apr. 2007.
- [6] C. Arndt, J. Karidas, and R. Busch, "Design and validation of a vehicle state estimator," in *Proc. 7th AVEC*, 2004, pp. 41–45.
- [7] L. Imsland, T. A. Johansen, T. I. Fossen, H. F. Grip, J. C. Kalkkuhl, and A. Suissa, "Vehicle velocity estimation using nonlinear observers," *Automatica*, vol. 42, no. 12, pp. 2091–2103, Dec. 2006.
- [8] F. Cheli, E. Sabbion, M. Pesce, and S. Melzi, "A methodology for vehicle sideslip angle identification: Comparison with experimental data," *Vehicle Syst. Dyn.*, vol. 45, no. 6, pp. 549–563, Jun. 2007.
- [9] T. A. Wenzel, K. J. Burnham, M. Blundell, and R. Williams, "Motion dual extended Kalman filter for vehicle state and parameter estimation," *Vehicle Syst. Dyn.*, vol. 44, no. 2, pp. 153–171, Feb. 2006.
- [10] A. Haddoun, M. El Hachemi Benbouzid, D. Diallo, R. Abdessemed, J. Ghouili, and K. Srairi, "Modeling, analysis, and neural network control of an EV electrical differential," *IEEE Trans. Ind. Electron.*, vol. 55, no. 6, pp. 2286–2294, Jun. 2008.
- [11] R. Babuska and H. Verbruggen, "An overview of fuzzy modeling for control," *Control Eng. Pract.*, vol. 4, no. 11, pp. 1593–1606, Nov. 1996.
- [12] D. Simon, "Kalman filtering for fuzzy discrete time dynamic systems," *Appl. Soft Comput.*, vol. 3, no. 3, pp. 191–207, Nov. 2003.
- [13] Y. Aoki, T. Uchida, and Y. Hori, "Experimental demonstration of body slip angle control based on a novel linear observer for electric vehicle," in *Proc. 31st IEEE IECON*, 2005, pp. 2620–2625.
- [14] C. S. Liu and H. Peng, "Road friction coefficient estimation for vehicle path prediction," *Vehicle Syst. Dyn.*, vol. 25, pp. 413–425, 1996. Suppl.
- [15] Y. Hori, "Future vehicle driven by electricity and control-research on four wheel motored 'UOT MARCH II,'" *IEEE Trans. Ind. Electron.*, vol. 51, no. 5, pp. 954–962, Oct. 2004.

- [16] P. J. T. Venhovens and K. Naab, "Vehicle dynamics estimation using Kalman filters," *Vehicle Syst. Dyn.*, vol. 32, no. 2/3, pp. 171–184, Aug. 1999.
- [17] M. C. Best, T. J. Gordon, and P. J. Dixon, "An extended adaptive Kalman filter for real-time state estimation of vehicle handling dynamics," *Vehicle Syst. Dyn.*, vol. 34, no. 1, pp. 57–75, Jul. 2000.
- [18] R. E. Kalman, "New result in linear filtering and prediction theory," *Trans. ASME, J. Basic Eng., Ser. D*, vol. 83, pp. 95–108, 1961.
- [19] C. Geng and Y. Hori, "Nonlinear body slip angle observer for electric vehicle stability control," in *Proc. 23rd EVS, 2007*, CD-ROM.
- [20] C. Geng, T. Uchida, and Y. Hori, "Body slip angle estimation and control for electric vehicle with in-wheel motors," in *Proc. 33rd IEEE IECON, 2007*, pp. 351–355.



Moulood Denai received the B.S. degree in electrical engineering from the University of Algiers, Algiers, Algeria, in 1982, and the Ph.D. degree in control engineering from The University of Sheffield, Sheffield, U.K., in 1988.

He is a Professor at Mohamed Boudiaf University of Science and Technology of Oran, Oran, Algeria. Currently, he is on research leave in the Department of Automatic Control and Systems Engineering, The University of Sheffield. His main fields of interest are intelligent control design; intelligent fault detection

in power systems; advanced control of power devices; modeling and control of electric power systems; modeling, simulation, and control design for efficiency optimization in the field of renewable energies such as solar and wind; investigation of power electronics interface for renewable energy systems; modeling and control of life science systems; data mining; and knowledge discovery for system modeling.



Cong Geng received the M.S. degree in vehicle engineering from Jilin University of Technology, Changchun, China, in 1996. She is currently working toward the Ph.D. degree at the University of Tokyo, Tokyo, Japan.

She joined the Department of Transportation and Traffic, Jilin University of Technology, as an Assistant Professor and became a Lecturer in 1999. She became a Lecturer at Beijing Jiaotong University, Beijing, China, in 2000. She is interested in vehicle dynamics analysis and control technology. Her studies

currently focus on advanced motion control of electric vehicles.



Yoichi Hori (S'81–M'83–SM'00–F'05) was born on July 14, 1955. He received the B.S., M.S., and Ph.D. degrees in electrical engineering from the University of Tokyo, Tokyo, Japan, in 1978, 1980, and 1983, respectively.

In 1983, he joined the Department of Electrical Engineering, University of Tokyo, as a Research Associate. He later became an Assistant Professor, an Associate Professor, and, in 2000, a Professor. During 1991–1992, he was a Visiting Researcher at the University of California, Berkeley. Since 2002,

he has been with the Institute of Industrial Science, University of Tokyo, as a Professor of electrical control system engineering in the Department of Informatics and Electronics. His research fields are control theory and its industrial applications to motion control, mechatronics, robotics, electric vehicles, etc.

Dr. Hori is a member of the Institute of Electrical Engineers of Japan (IEE-Japan), Japan Society of Mechanical Engineering, Society of Instrument and Control Engineers, Robotics Society of Japan, Society of Automobile Engineers of Japan, and Japan Society for Simulation Technology, among others. He was the Treasurer of IEEE Japan Council and Tokyo Section during 2001–2002. He is currently an AdCom member of the IEEE Industrial Electronics Society. He was the Vice President of the IEE-Japan Industry Applications Society during 2004–2005. He is the Chairman of the Energy Capacitor Storage System Forum and the Motor Technology Symposium of the Japan Management Association. He was the winner of the Best Paper Awards from the IEEE TRANSACTIONS ON INDUSTRIAL ELECTRONICS in 1993 and 2001.



Lotfi Mostefai received the M.S. degree in electrical control engineering from Mohamed Boudiaf University of Science and Technology of Oran, Oran, Algeria, in 2002. He is currently working toward the Ph.D. degree at Mohamed Boudiaf University of Science and Technology of Oran.

He lectured on "control engineering" and "microprocessors and microcontrollers in industrial applications" at the University Moulay Tahar, Saïda, Algeria. He was with the Hori Laboratory, Institute of Industrial Science, University of Tokyo, Tokyo,

Japan, as a Research Student in 2006. His research interests are optimal and robust control, motion control systems, smart materials and their applications, automotive engineering, and renewable energies.